Supplement of

Secondary OH reactions of aromatics-derived oxygenated organic molecules lead to plentiful highly oxygenated organic molecules within an intraday OH exposure

Yuwei Wang[1], Yueyang Li[1], Gan Yang[1], Xueyan Yang[1], Yizhen Wu[1], Chuang Li[1], Lei Yao[1,2], Hefeng, Zhang[3*], Lin Wang[1,2,4,5,6] *

[1] Shanghai Key Laboratory of Atmospheric Particle Pollution and Prevention (LAP[3]), Department of Environmental Science and Engineering, Jiangwan Campus, Fudan University, Shanghai 200438, China

[2] Shanghai Institute of Pollution Control and Ecological Security, Shanghai 200092, China

[3] State Environmental Protection Key Laboratory of Vehicle Emission Control and Simulation, Vehicle Emission Control Center of Ministry of Ecology and Environment, Chinese Research Academy of Environmental Sciences, Beijing 100012, China

[4] IRDR International Center of Excellence on Risk Interconnectivity and Governance on Weather/Climate Extremes Impact and Public Health, Fudan University

[5] National Observations and Research Station for Wetland Ecosystems of the Yangtze Estuary, Shanghai, China

[6] Collaborative Innovation Center of Climate Change, Nanjing, 210023, China

** Corresponding Author: H.Z., email, zhanghf@craes.org.cn; phone, +86-10-84915586*

L.W., email, lin_wang@fudan.edu.cn; phone, +86-21-31243568

Contents of this file:

12 pages

Table S1-S2

Figures S1-S5

Text S1-S2

Text S1. Calculation of the nominal relative molar yields of HOMs

Following a previous study (Garmash et al., 2020), the change in HOM concentration in time is defined as HOM production rate minus HOM loss rate:

$$\frac{d[HOM]}{dt} = \gamma k_{VOC+OH}[VOC][OH] - k_{loss}[HOM]$$

where γ denotes the molar HOM yield, k_{loss} is the loss coefficient of HOMs, k_{VOC+OH} is the OH oxidation reaction coefficient of the VOC precursor, and $[HOM]$, $[VOC]$, and $[OH]$ are the concentrations of HOMs, VOC precursors, and OH radicals at the exit of PAM OFR, respectively (Garmash et al., 2020).

By assuming a steady state was achieved at the exit of PAM OFR, the concentration of every compound was constant and $d[HOM]/dt$ should be 0. Then the molar HOM yield, γ, was the fraction of reacted VOC molecules that was converted into HOMs and then calculated as:

$$\gamma = \frac{k_{loss}[HOM]}{k_{VOC+OH}[VOC][OH]} \qquad \textbf{(I)}$$

In laboratory experiments, as mentioned in the manuscript, an absolute molar HOM yield was unable to be calculated because the sampling efficiency of the nitrate CIMS was difficult to be estimated. However, k_{loss} should be constant in all of the experiments, as the loss coefficient of HOMs in the PAM OFR and sampling efficiency should not change. Therefore, the variation tendency of $[HOM]/(k_{VOC+OH}[VOC][OH])$ along with the changes of OH exposure should be identical as γ.

On the other hand, concentrations of HOMs at the exit of PAM OFR, $[HOM]$, can be calculated as:

$$[HOM] = C \times \frac{S(HOM)}{\sum_{n=0,2}(NO_3^-)\cdot(HNO_3)_n} \qquad \textbf{(II)}$$

where C (in units of cm^{-3}) is the calibration factor corrected by the transmission efficiency of the nitrate CIMS (Ehn et al., 2014). To avoid potential uncertainties in the calibration, arbitrary signals of compounds measured the mass spectrometers normalized by the reagent ions were utilized, since we were not going to calculate the absolute value for laboratory experiments.

Text S2. Estimation of the OH reaction rate of $C_{18}H_{26}O_8$

The proposed structure of $C_{18}H_{26}O_8$ is shown in Figure S5 to help understanding but the potential cis-trans isomerism is not considered in this study.

A reaction rate constant for a OH-initiated reaction is defined in terms of a summation of partial rate constants for OH addition and H-atom abstraction by OH. There are two -CH=C< structure units in the $C_{18}H_{26}O_8$. The rate constant for OH addition to -CH=C< bond depends on the number, identity and position of substituent groups around it, of which the effects on the rate constants are quantitatively shown as substituent factors. For isolated C=C bonds in the alkenes, Peeters et al. defined site-specific parameters for addition of OH, i.e., $k_{pri\text{-}add}$, $k_{sec\text{-}add}$, and $k_{tert\text{-}add}$, respectively, to form primary, secondary and tertiary β-hydroxyalkyl radicals (Peeters et al., 2007). According to results of a previous study (Jenkin et al., 2018), $k_{sec\text{-}add}$, and $k_{tert\text{-}add}$ at 298 K are 2.63×10^{-11} cm^3 $molecule^{-1}$ s^{-1} and 5.15×10^{-11} cm^3 $molecule^{-1}$ s^{-1}, respectively. The -CH=C< structure units have two sites where OH can be attached to form a secondary and a tertiary β-hydroxyalkyl radical, respectively. One of the sites is neighboring to the >CH-O-O-CH< functional group and the other one to the bicyclic peroxide functional group. To our best knowledge, the activating effect on OH reactivity of the >CH-O-O-CH< functional group and bicyclic peroxide functional group was not previously reported. In a previous work, the activating effect of -OOH is suggested to be identical to -OH and -OOR (Jenkin et al., 2018). Therefore, the >CH-O-O-CH< peroxy linkage functional group and bicyclic peroxide functional group are assumed to have the same activating effects as -CH_2OOH, -CH(OOH), and -C(OOH)<, whose substituent factors for the addition OH to C=C bonds are 1.2. Hence, the OH addition reaction rate constant is estimated to be 9.34×10^{-11} cm^3 $molecule^{-1}$ s^{-1}.

Abstraction of H atoms is typically much slower than OH addition. Previous studies also assumed that the abstraction of H atoms from the aromatic ring is negligible under atmospheric conditions based on reported data for the reaction of OH with benzene (Calvert et al., 2002). The rate coefficient for H-atom abstraction from OH group in phenol is around 2.6×10^{-12} cm^3 $molecule^{-1}$ s^{-1} at 298 K (Atkinson et al., 1992; Berndt and Böge, 2003; Coeur-Tourneur et al., 2006; Olariu et al., 2002). This is already around a factor of 20 greater than estimated values for abstraction from -OH groups in aliphatic compounds, which is around 1.4×10^{-13} cm^3 $molecule^{-1}$ s^{-1} at 298 K if no influences from neighboring substituent groups are considered (Jenkin et al., 2018; Kwok and Atkinson, 1995). Here, we only considered the H-atom abstraction on the -CH=C< structure units in $C_{18}H_{26}O_8$ as the H-atom abstraction on other positions is too slow. The group rate coefficient for H-atom abstraction from tertiary carbon is 1.49×10^{-12} cm^3 $molecule^{-1}$ s^{-1} and the substituent factor related to H-atom abstraction reactions of OH adjacent to this double bond is 6.2. In addition, the empirical ring-strain factor has to be applied on the H-atom abstraction because of the C=C bond is in a 7-member ring structure, which is 1.12. Hence, the H-abstraction rate constant is calculated to be 1.03×10^{-11} cm^3 $molecule^{-1}$ s^{-1}. No adjustments were made for potential impacts of ring strain effects on the OH addition rate constant as suggested by Jenkin et al.(2018).

As a final step, because there are two -CH=C< structure units in $C_{18}H_{26}O_8$, the total OH reaction rate constant needs to be multiplied by 2, which is 2.07×10^{-10} cm^3 $molecule^{-1}$ s^{-1}.

The distribution of errors ($\log k_{calc}/k_{obs}$, where k_{calc} and k_{obs} are the calculated and observed OH reaction rate, respectively) for cyclic alkenes of the SAR methods updated by Jenkin et al. has a root mean squared error (RMSE) of 0.11 and a mean absolute error (MAE) of 0.082 (Jenkin et al., 2018), corresponding to an uncertainty within $^{+28.8}_{-23.3}$% for the calculated OH reaction rate constants of

$C_{18}H_{26}O_8$. Therefore, the total OH reaction rate constant of $C_{18}H_{26}O_8$ is in the range of 1.61 – 2.67 $\times 10^{-10}$ cm^3 $molecule^{-1}$ s^{-1}.

Table S1. Summary of experimental conditions.

No.	Initial concentration of 1,3,5-TMB (ppb)	O_3 concentration (ppb)**	NO concentration (ppb)	NO_2 concentration (ppb)	Estimated OH exposure based on the precursor consumption ($\times 10^{10}$ molecule cm^{-3} s)
1	54.6	451	0	0	1.85
2	58.9	455	0	0	1.12
3	62.7	467	0	0	0.52
4	38.4	434	0	0	4.40
5	39.9	441	0	0	4.09
6	41.2	445	0	0	3.48
7	41.9	453	0	0	2.87
8	43.8	461	0	0	2.19
9	45.6	471	0	0	1.33
10	46.8	479	0	0	0.63
11	47.7	483	0	0	0.59
12	48.1	482	0	0	4.49
13	48.4	427	0	0	3.98
14	47.8	434	0	0	3.59
15	47.9	443	0	0	3.15
16	48.9	451	0	0	2.68
17	49.5	458	0	0	1.89
18	49.7	467	0	0	1.13
19	50.3	480	0	0	0.53
20	28.9	428	0	0	4.87
21	31.3	428	0	0	4.81
22	32.5	429	0	0	4.41
23	33.4	440	0	0	3.81
24	33.9	448	0	0	3.25
25	34.4	455	0	0	2.38
26	34.8	466	0	0	1.61
27	49.7	424	0	0	4.19
28	50.6	434	0	0	3.78
29	50.0	441	0	0	3.43
30	50.5	448	0	0	2.97
31	51.4	457	0	0	2.44
32	51.6	464	0	0	1.78
33	52.5	477	0	0	1.06
34	46.6	429	0	0	4.35
35	47.3	436	0	0	3.85
36	47.9	442	0	0	3.52
37	48.8	451	0	0	3.01
38	50.0	460	0	0	2.56

39	50.6	466	0	0	1.81
40	51.6	477	0	0	1.16
41	29.7	864	2.01	60	3.11
42	37.1	856	1.85	64	2.89
43	44.6	853	1.86	67	2.73
44	52.3	854	1.76	68	2.57
45	59.7	856	1.71	70	2.41
46	67.8	858	1.65	71	2.26
47	26.8	860	1.96	65	3.19
48	31.5	874	1.93	68	3.09
49	39.4	874	1.84	70	2.86
50	46.7	879	1.76	72	2.70
51	55.3	881	1.70	73	2.53
52	64.8	880	1.63	74	2.36
53	73.3	864	1.61	75	2.19
54	84.1	883	1.57	78	2.06
55	29.2	714	4.81	104	3.98
56	35.5	703	4.82	111	3.77
57	16.7	695	5.32	109	4.18
58	22.9	697	5.21	112	4.14
59	29.6	699	4.91	117	3.84
60	36.0	698	4.70	119	3.62
61	41.4	698	4.52	122	3.43
62	46.5	688	4.61	128	3.31
63	52.4	692	4.47	130	3.18
64	25.0	675	5.46	125	3.89
65	30.9	683	5.32	127	3.68
66	36.8	688	5.02	131	3.47
67	42.3	688	4.89	132	3.33
68	48.5	688	4.64	134	3.22

** O_3 concentrations were stable values measured after the lights were turned on.

Table S2. Molecular formulae and molar masses of observed HOM monomers and dimers in the NO_x-free experiments, along with their relative contributions to the total HOMs signals when OH exposure equaled 2.38×10^{10} molecules cm^{-3} s (Exp. 25).

No.	Molecular formula	Molar mass	Contributions to total HOMs signals (%)
1	$C_7H_8O_7$	204.0270	0.19
2	$C_8H_{12}O_6$	204.0634	0.20
3	$C_7H_{10}O_7$	206.0427	0.39
4	$C_9H_{12}O_6$	216.0634	0.40
5	$C_9H_{13}O_6$	217.0712	0.15
6	$C_8H_{10}O_7$	218.0427	1.22
7	$C_9H_{14}O_6$	218.0790	1.17
8	$C_8H_{11}O_7$	219.0505	0.24
9	$C_9H_{15}O_6$	219.0869	0.14
10	$C_7H_8O_8$	220.0219	0.14
11	$C_8H_{12}O_7$	220.0583	0.90
12	$C_9H_{16}O_6$	220.0947	0.68
13	$C_7H_{10}O_8$	222.0376	0.45
14	$C_8H_{14}O_7$	222.0740	0.22
15	$C_9H_{12}O_7$	232.0583	0.72
16	$C_9H_{13}O_7$	233.0661	0.24
17	$C_9H_{14}O_7$	234.0740	6.02
18	$C_9H_{15}O_7$	235.0818	2.35
19	$C_9H_{16}O_7$	236.0896	3.72
20	$C_9H_{12}O_8$	248.0532	0.75
21	$C_9H_{13}O_8$	249.0610	0.11
22	$C_9H_{14}O_8$	250.0689	2.30
23	$C_9H_{15}O_8$	251.0767	2.15
24	$C_9H_{16}O_8$	252.0845	4.08
25	$C_9H_{13}O_9$	265.0560	0.36
26	$C_9H_{14}O_9$	266.0638	1.34
27	$C_9H_{15}O_9$	267.0716	0.95
28	$C_9H_{16}O_9$	268.0794	2.44
29	$C_9H_{12}O_{10}$	280.0430	0.23
30	$C_9H_{14}O_{10}$	282.0587	0.54
31	$C_9H_{15}O_{10}$	283.0665	0.27
32	$C_9H_{16}O_{10}$	284.0743	0.39
33	$C_9H_{12}O_{11}$	296.0380	0.16
34	$C_{18}H_{26}O_8$	370.1628	0.38
35	$C_{18}H_{24}O_9$	384.1420	0.31
36	$C_{18}H_{26}O_9$	386.1577	0.37
37	$C_{17}H_{24}O_{10}$	388.1369	0.31
38	$C_{18}H_{24}O_{10}$	400.1369	0.80
39	$C_{18}H_{26}O_{10}$	402.1526	9.49
40	$C_{18}H_{28}O_{10}$	404.1682	4.62

41	$C_{18}H_{24}O_{11}$	416.1319	0.82
42	$C_{18}H_{26}O_{11}$	418.1475	2.99
43	$C_{18}H_{28}O_{11}$	420.1632	7.67
44	$C_{18}H_{24}O_{12}$	432.1268	0.86
45	$C_{18}H_{26}O_{12}$	434.1424	6.44
46	$C_{18}H_{28}O_{12}$	436.1581	9.17
47	$C_{18}H_{30}O_{12}$	438.1737	1.49
48	$C_{18}H_{24}O_{13}$	448.1217	0.67
49	$C_{18}H_{26}O_{13}$	450.1373	3.26
50	$C_{18}H_{28}O_{13}$	452.1530	6.49
51	$C_{18}H_{30}O_{13}$	454.1686	1.15
52	$C_{18}H_{24}O_{14}$	464.1166	0.53
53	$C_{18}H_{26}O_{14}$	466.1323	1.87
54	$C_{18}H_{28}O_{14}$	468.1479	3.16
55	$C_{18}H_{30}O_{14}$	470.1636	1.64
	Total monomer		35.5
	Total dimer		64.5

(a)

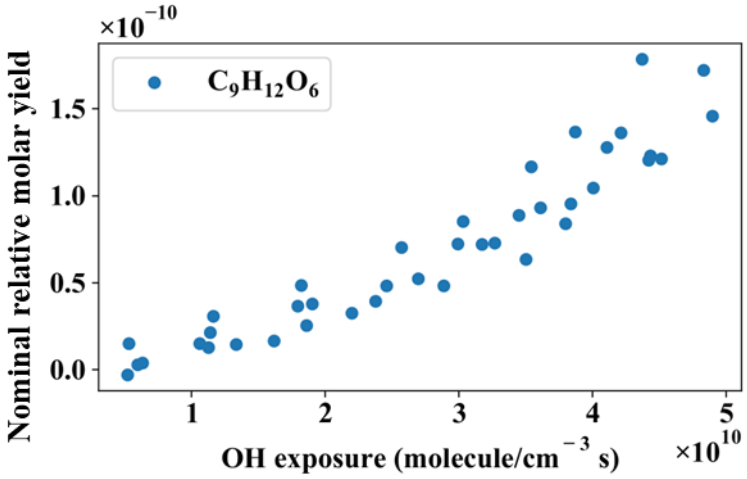

(b)

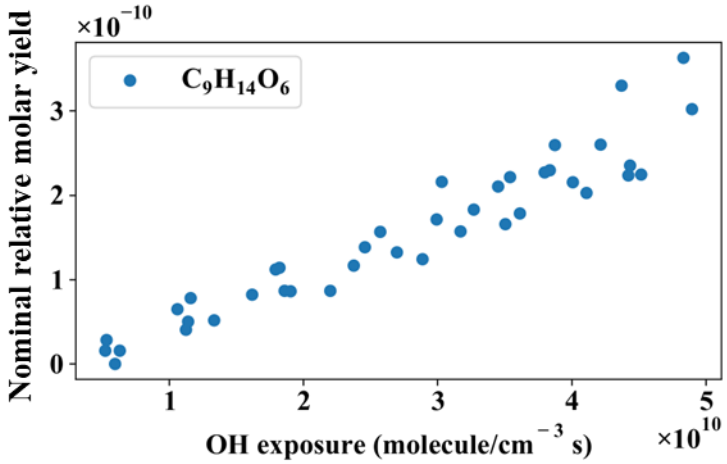

(c)

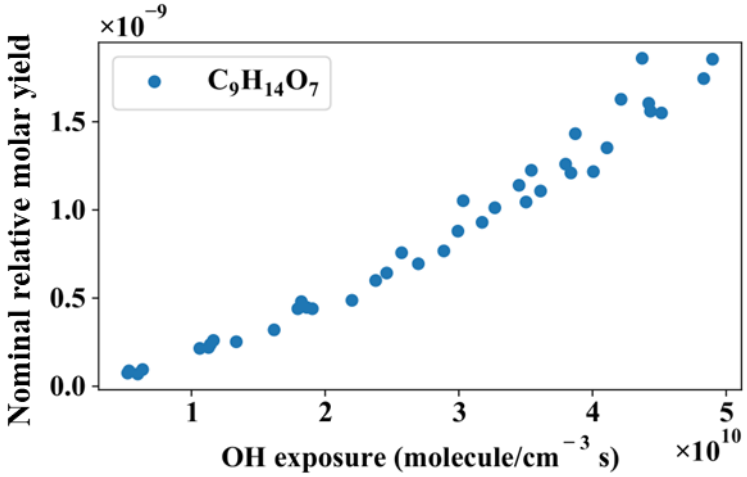

Figure S1. Nominal relative molar yields of (a) $C_9H_{12}O_6$, (b) $C_9H_{14}O_6$, and (c) $C_9H_{14}O_7$ plotted as a function of OH exposure in the PAM OFR.

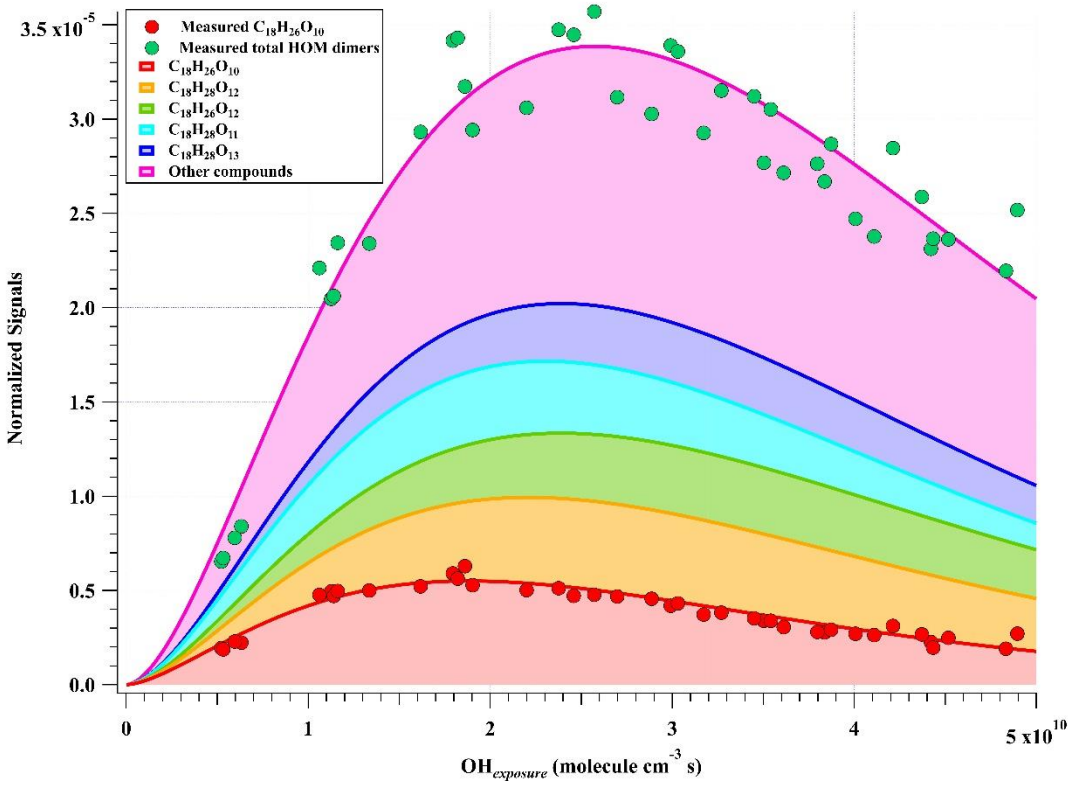

Figure S2. Normalized signals of HOM dimers versus OH exposure, fitted via a gamma function and shown in a stacked manner.

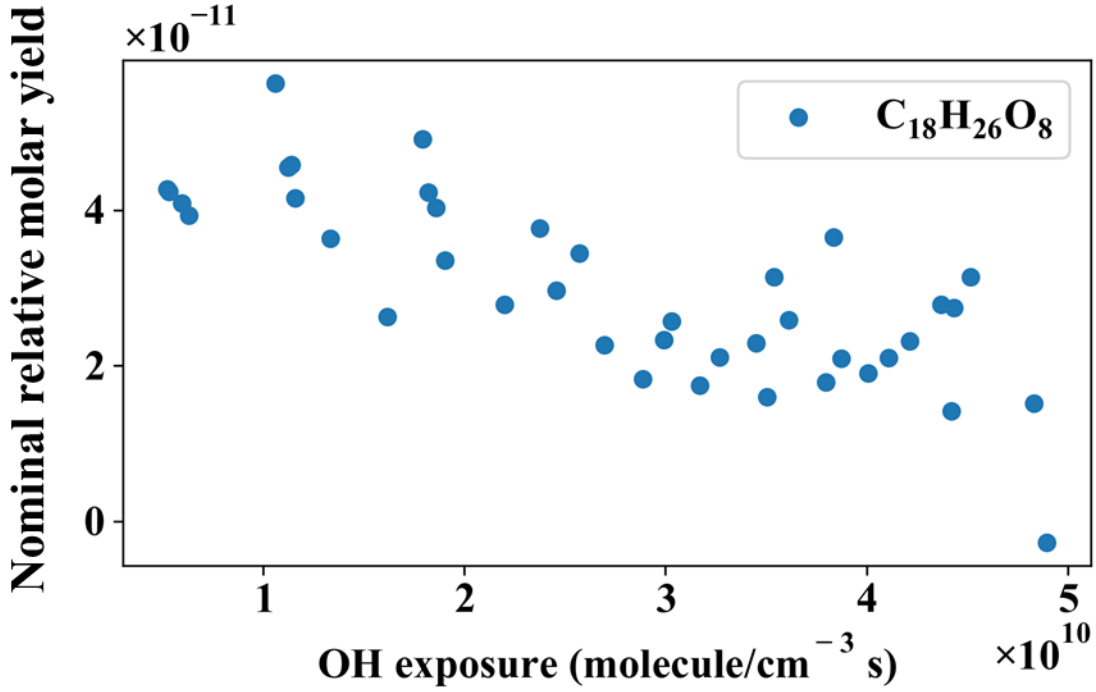

Figure S3. The nominal relative molar yield of $C_{18}H_{26}O_8$ as a function of OH exposure in the OH-initiated 1,3,5-TMB oxidation experiments.

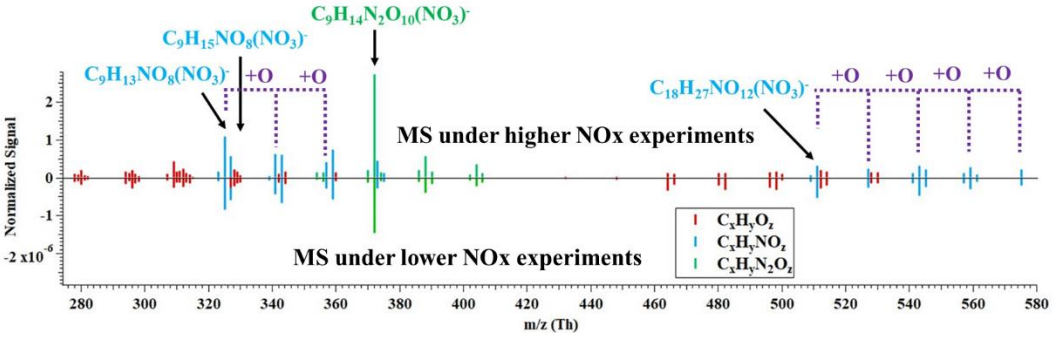

Figure S4. Mass spectrometry of HOMs detected by nitrate CIMS in the NO_x experiments, presented with the averaged normalized signals in 1.8 ppb NO + 70 ppb NO_2 and 4.8 ppb NO + 120 ppb NO_2 experiments. For comparison, the mass spectrometry under lower NOx experiments is shown in opposite values.

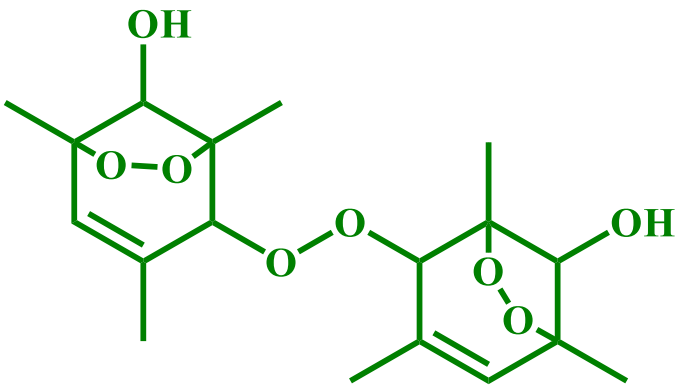

Figure S5. A plausible structure of $C_{18}H_{26}O_8$. The potential cis-trans isomerism is not shown.

References

Atkinson, R., Aschmann, S. M. and Arey, J.: Reactions of hydroxyl and nitrogen trioxide radicals with phenol, cresols, and 2-nitrophenol at 296 +- 2 K, Environ. Sci. Technol., 26(7), 1397–1403, doi:10.1021/es00031a018, 1992.

Berndt, T. and Böge, O.: Gas-phase reaction of OH radicals with phenol, Phys. Chem. Chem. Phys., 5(2), 342–350, doi:10.1039/b208187c, 2003.

Calvert, J. G., Becker, K. H., Kamens, R., Seinfeld, J., Wallington, T. J. and Yarwood, G.: The Mechanisms of Atmospheric Oxidation of the Aromatic Hydrocarbons., 2002.

Coeur-Tourneur, C., Henry, F., Janquin, M. A. and Brutier, L.: Gas-phase reaction of hydroxyl radicals with m-, o- and p-cresol, Int. J. Chem. Kinet., 38(9), 553–562, doi:10.1002/kin.20186, 2006.

Ehn, M., Thornton, J. A., Kleist, E., Sipilä, M., Junninen, H., Pullinen, I., Springer, M., Rubach, F., Tillmann, R., Lee, B., Lopez-Hilfiker, F., Andres, S., Acir, I. H., Rissanen, M., Jokinen, T., Schobesberger, S., Kangasluoma, J., Kontkanen, J., Nieminen, T., Kurtén, T., Nielsen, L. B., Jørgensen, S., Kjaergaard, H. G., Canagaratna, M., Maso, M. D., Berndt, T., Petäjä, T., Wahner, A., Kerminen, V. M., Kulmala, M., Worsnop, D. R., Wildt, J. and Mentel, T. F.: A large source of low-volatility secondary organic aerosol, Nature, 506(7489), 476–479, doi:10.1038/nature13032, 2014.

Garmash, O., Rissanen, M. P., Pullinen, I., Schmitt, S., Kausiala, O., Tillmann, R., Zhao, D., Percival, C., Bannan, T. J., Priestley, M., Hallquist, Å. M., Kleist, E., Kiendler-Scharr, A., Hallquist, M., Berndt, T., McFiggans, G., Wildt, J., Mentel, T. F. and Ehn, M.: Multi-generation OH oxidation as a source for highly oxygenated organic molecules from aromatics, Atmos. Chem. Phys., 20(1), 515–537, doi:10.5194/acp-20-515-2020, 2020.

Jenkin, M. E., Valorso, R., Aumont, B., Rickard, A. R. and Wallington, T. J.: Estimation of rate coefficients and branching ratios for gas-phase reactions of OH with aliphatic organic compounds for use in automated mechanism construction., 2018.

Kwok, E. S. C. and Atkinson, R.: Estimation of hydroxyl radical reaction rate constants for gas-phase organic compounds using a structure-reactivity relationship: An update, Atmos. Environ., 29(14), 1685–1695, doi:10.1016/1352-2310(95)00069-B, 1995.

Olariu, R. I., Klotz, B., Barnes, I., Becker, K. H. and Mocanu, R.: FT-IR study of the ring-retaining products from the reaction of OH radicals with phenol, o-, m-, and p-cresol, Atmos. Environ., 36(22), 3685–3697, doi:10.1016/S1352-2310(02)00202-9, 2002.

Peeters, J., Boullart, W., Pultau, V., Vandenberk, S. and Vereecken, L.: Structure-activity relationship for the addition of OH to (poly)alkenes: Site-specific and total rate constants, J. Phys. Chem. A, 111(9), 1618–1631, doi:10.1021/jp066973o, 2007.